IEEE Robotics and Automation Letters (RA-L) paper, presented at ICRA 2024, Yokohama, Japan. Cite as RA-L paper.

Task-based Human-Robot Collaboration Control of Supernumerary Robotic Limbs for Overhead Tasks

Zhixin Tu, Yijun Fang, Yuquan Leng, and Chenglong Fu

***Abstract*—Supernumerary robotic limbs (SRLs) are novel wearable robots that can be used to augment human operating ability in completing some difficult and complex tasks. In this work, a task-based human-SRLs collaboration control method for overhead tasks is developed. It is autonomous and safe without the need for active commands and previous data. A task model is proposed to model the human-SRLs collaboration process that features different task states and state transition conditions. Specifically, the overhead task process is modeled as a finite state machine (FSM) with four task states, three trigger events, and three SRLs actions. The real-time measured human motion data is utilized to trigger the task state transition and estimate the task parameters, which are the constraints for SRLs motion planning. The proposed admittance control with adjustable parameters allows SRLs to behave like spring-damping systems with different characteristics in different states and actions. The admittance control enhances the safety and reliability of the human-SRLs interaction. Finally, the effectiveness of the proposed control method for overhead tasks is further validated on a prototype of the human-SRLs system with two subjects under different installation heights. Trigger events and task parameters are successfully detected and estimated during the task process to trigger the coordination actions of SRLs. The results demonstrate that the task-based collaboration method is useful for overhead tasks with different task parameters.**

***Index Terms*—Wearable robotics, human-robot collaboration, human performance augmentation, supernumerary robotic limbs (SRLs).**

I. Introduction

SUPERNUMERARY robotic limbs (SRLs) are a novel kind of wearable robots developed as extended independent limbs for human augmentation [1]–[3]. Different from exoskeletons [4], prostheses [5], and other wearable robots, SRLs are regarded as the additional arms or legs to be applied to augment humans' capabilities. They can assist humans in performing complex and intensive tasks by providing additional strength, flexibility, and support, which can be useful in tight or confined spaces (e.g. aircraft component assembly [6]).

The main role of SRLs is to help humans with tasks that cannot be done by one single person. This requires a well-organized human-SRLs collaboration. Ideally, this collaboration should be able to handle complex tasks under varying task parameters. In human-human collaboration, verbal and physical communication among humans ensures a shared understanding of intentions, task-knowledge, and coordination of actions [7]. However, unlike humans who can comprehend the meaning behind continuous speech and physical gestures, SRLs as non-intelligent agents lack the capability to understand and interpret these forms of communication accurately. Although humans can perceive the position and force of SRLs through inherent vision and haptic feedback [6], [8], human intentions and some task-related knowledge (in terms of task state and task parameters) cannot be easily transmitted to SRLs due to the lack of neuromuscular connection in the heterogeneous form. Therefore, effectively communicating task knowledge and intentions between the human and SRLs is a key challenge in human-SRLs collaboration control.

In the existing literature, various control methods have been developed for human-SRLs system. They can be briefly divided into two groups, active control [9]–[11] and reactive control [12]–[14]. Active control means that the human expresses his control commands actively to control the motion of SRLs. Generally, it redirects unused DoFs (in terms of task-irrelevant movement) of the human to the DoFs of SRLs. The control signals mainly include body movements [9], [10], electromyography (EMG) [11], etc. Guggenheim *et al.* [10] exploited the combination of force at the fingertips to communicate the action primitives to the SRL. In [11], the EMG signals of the torso muscles were remapped to control the two-DoF SRLs. This solution is effective for some simple tasks with limited DoFs. Active control for complex tasks with multiple DoFs is currently limited by the precision of the redirected DoFs and the cognitive load on the human [1].

Reactive control means that SRLs do not depend on explicit commands but generates the corresponding motion by understanding human behavior, intentions, and the task state. To date, teaching-data-based reactive control (TDRC) has been introduced in some studies [12]–[14]. In [12], a SRLs prototype was designed to assist humans in overhead tasks, using the partial least square (PLS) algorithm to train a large number of manual teaching data to generate the trajectory. Wu and Asada [14] utilized the data of human grasping actions to train a prediction model. This trained model was then applied to control the supernumerary robotic fingers in a semi-autonomous manner. In this method, the motion pattern of SRLs is usually based on a predefined model and SRLs can be able to coordinate with humans in a natural and intuitive way without explicit commands. TDRC has obtained some

This work was supported in part by the National Natural Science Foundation of China under Grants U1913205, the Stable Support Plan Program of Shenzhen Natural Science Fund under Grant 20200925174640002, and the Science, Technology and Innovation Commission of Shenzhen Municipality under Grant ZDSYS20200811143601004. (*Corresponding author: Chenglong Fu.*)

The authors are with the Shenzhen Key Laboratory of Biomimetic Robotics and Intelligent Systems and Guangdong Provincial Key Laboratory of Human-Augmentation and Rehabilitation Robotics in Universities, Southern University of Science and Technology, Shenzhen 518055, China (email: 12131094@mail.sustech.edu.cn; 12011301@mail.sustech.edu.cn; lengyq@sustech.edu.cn; fucl@sustech.edu.cn)

Digital Object Identifier (DOI): see top of this page.

IEEE Robotics and Automation Letters (RA-L) paper, presented at ICRA 2024, Yokohama, Japan. Cite as RA-L paper.

achievements in human intention recognition [12]–[14], but it requires a large amount of high-dimensional demonstration data from the user to guarantee its feasibility, which hinders its application in complex situations. Since the teaching data is always implicit and collected from a limited set of task parameters, the quantitative task parameters during the task process (e.g., installation height [12], drilling position [13]) can not be estimated, further limiting its deployment in varying working environments.

To address the limitations of current control methods in adapting to complex environments and varying task parameters, a task-based collaboration control method is proposed. The aim of this method is to construct a communication channel for task-knowledge and intention in order to facilitate effective and autonomous collaboration for a specific complex task with varying task parameters. To achieve this, a task model is proposed to fully describe the task process and generally coordinate the human-SRLs behavior. The real-time measurement of human motion allows SRLs to observe the human actions, understand the human intention and estimate the task-knowledge. The proposed method is different from the existing studies that utilized the human motion data to teleoperate the mobile robots [15] or improve the human ergonomics in human-robot collaboration [16]. As far as we are aware, this work is the first to introduce a task model driven by human motion data for the collaboration control of SRLs to extract the human intention and task parameters.

Overhead tasks for ceiling installation [6], [12], [17] are representative applications of SRLs, as shown in Fig. 1(c). The specific task can not be achieved by a single person, since if the natural hands are occupied to support the ceiling, the installation is impossible. Previous studies on overhead tasks have primarily been confined to a single scene [17] or the SRLs control with fixed task parameters [12]. However, the collaboration control of varying ceiling heights throughout the entire task process has not received sufficient attention. In this work, a finite state machine (FSM)-based task model is proposed to coordinate the human-SRLs behavior. The ceiling installation height and the task state can be estimated by the human motion data, providing a comprehensive description of the overhead tasks. Since the motion of human limbs and task parameters are considered in the SRLs motion planning and control, the human-SRLs collaboration will be safer and more robust. Safety and robustness are also the key points of the human-SRLs interaction. The main contributions of this paper are listed as follows:

(i) A task model driven by human motion data is built to communicate the intention and task-knowledge between the human and SRLs, which can guarantee the autonomy and safety of the human-SRLs collaboration for complex tasks under different task parameters without the need of an active control or previously recorded data.

(ii) The proposed method is demonstrated for overhead tasks. Experiments are performed to validate the effectiveness of the proposed method with different task parameters. The experiment results are demonstrated and discussed in detail.

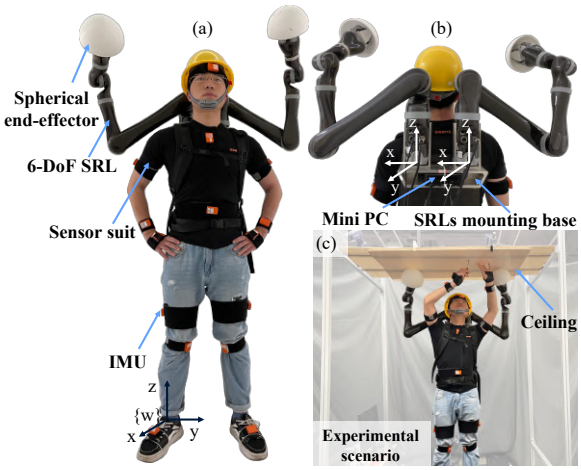

Fig. 1. Human-SRLs hardware system configuration and the experimental scenario for overhead tasks. (a) The front view of the hardware system. The black coordinate system is the world frame $\{w\}$, with the origin of the frame defined at the human operator's right heel. (b) The rear view of the hardware system. The white coordinate systems are the base frames of the SRLs. (C) The experimental scenario for overhead tasks. The experimental scenario was built by eight aluminum profiles in which the installation height can be adjusted by moving the horizontal profiles along the four vertical aluminum profiles.

II. Methods

Fig. 2 illustrates the control framework of the human-SRLs system for overhead tasks. It is composed of three parts: (A) IMU-based human motion capture, (B) overhead task model, (C) SRLs control strategy. The first part utilizes multiple IMUs to obtain the real-time motion of human. Then the motion data which can reflect the human intention is used to drive the proposed task model to identify the task states Q_i and estimate the task parameters, such as installation height h and supporting points $P^w_{support}$. Finally, based on the task model and the task parameters, the SRLs controller generates the motion trajectories and adjusts the admittance control parameters accordingly to collaborate with the human operator.

A. IMU-based Human Motion Capture System

From human motion data, it is possible to extract the human intention and task-related information, which are important in human-SRLs collaboration tasks. IMUs can be used to measure the acceleration and orientation of the body segments, then the motion of the human can be accurately reconstructed by fusing the body kinematics and acceleration integration. In this paper, the commercial system Xsens MVN (Xsens, Netherlands) [18] is adopted to measure the real-time motion of the human operator with a frequency of 60 Hz. A sensor suit composed of 17 wireless IMUs (MTw, Xsens, Netherlands) is worn by the human operator [18], as shown in Fig. 1. The origin of each reference frame is placed at the proximal joint center of each segment. For example, the coordinate of the hand is defined at the proximal joint of the hand, i.e. the wrist. Therefore, the position of each segment i at time step k in world frame $\{w\}$ can be described as the position of the origin of frame $\{i\}$ denoted by

$$P^w_{i,k} = [x^w_{i,k}, y^w_{i,k}, z^w_{i,k}] \in \mathbb{R}^3. \quad (1)$$

IEEE Robotics and Automation Letters (RA-L) paper, presented at ICRA 2024, Yokohama, Japan. Cite as RA-L paper.

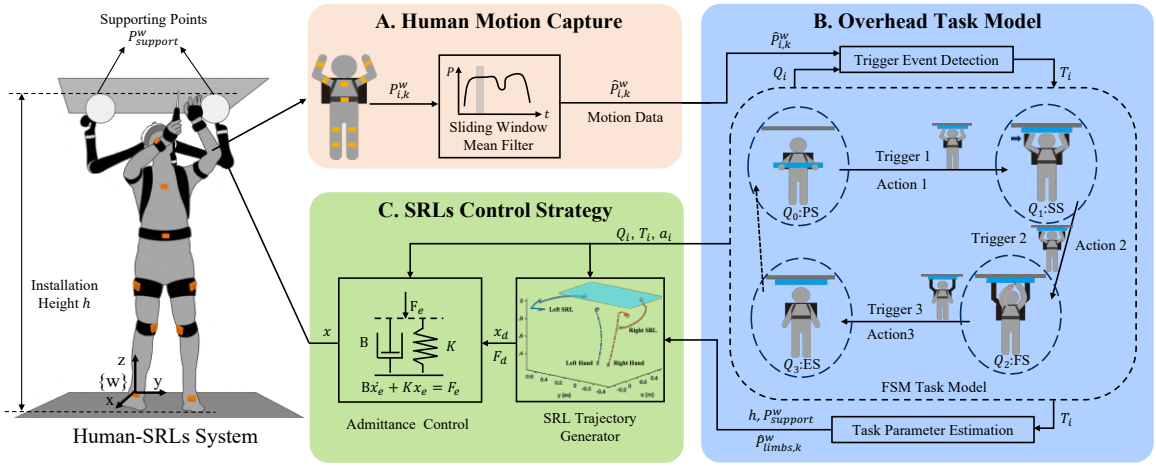

Fig. 2. Overview of the collaboration control framework of human-SRLs system for overhead tasks. (A) $P^w_{i,k}$ is the raw data of human motion data, and $\hat{P}^w_{i,k}$ is the filtered human motion data. (B) Q_i, T_i, and a_i represent the task state Q_i, trigger event T_i, and SRLs action a_i, respectively. (C) $x_d \in \mathbb{R}^6$ and $x \in \mathbb{R}^6$ are the planned motion trajectory generated by SRLs trajectory generator and the actual trajectory calculated by the admittance controller in task space, respectively.

The time-series motion data is processed using a Sliding Window Mean filter with a window length equivalent to half the frequency of the motion data, which is 30. This filter can smooth the data and reduce the measurement noise. Then the filtered data $\hat{P}^w_{i,k}$ is used as input of the task model.

B. Overhead Task Model

1) FSM Task Modeling: The task model of human-SRLs collaboration describes a series of sequential human-SRLs actions required to achieve the task. This includes the task states, task parameters, and corresponding state transition timings. The task model can generally fully define tasks with the similar process which facilitates the application in practice.

The human operator often leads the process of the human-SRLs task and decides the state of the task, then the SRLs refer to the state and state transition to timely generate assistive actions. In overhead tasks, ceiling installation is an example of a collaboration task containing a sequence of human-SRLs actions. The selected overhead task of installing one ceiling proceeds as follows: (i) the human operator pre-places the ceiling to the installation plane and adjusts the ceiling to align with the installation holes; (ii) the SRLs assist the human operator to support the ceiling; (iii) the human operator uses the screwdriver to fix the ceiling; (iv) after the ceiling is fixed, the human limbs and the SRLs go back to the starting position.

The human-SRLs actions can also be divided into the different states of the task according to the task process. In each state and state transition, the SRLs need to generate different actions. The FSM-based overhead task model can be expressed as a tuple that contains the task states space Q, trigger event set T, SRLs action set a, and state transition function $\delta(Q_i, T_{i+1})$:

$$\text{FSM} =< Q, T, a, \delta > . \tag{2}$$

As shown in Fig. 3, the FSM model has four different human-SRLs states just as the four human-SRLs actions of the task process, "prepare state" (PS), "supporting state" (SS), "fixing state" (FS), and "end state" (ES), that constitutes the state space Q, denoted by

$$Q = \{Q_0, Q_1, Q_2, Q_3\} = \{PS, SS, FS, ES\}. \tag{3}$$

(i) In PS, the human operator is about to start the task by holding the ceiling; PS is the initial state of the task. (ii) In SS, the human operator can fine-tune the position of the ceiling to align with the holes. (iii) In FS, the ceiling is supported by the SRLs, while the human operator is fixing the ceiling. (iv) In ES, the task is completed when the SRLs and the human limbs go back to the original position. ES is the final state of the task.

The state transitioning for the FSM task model is controlled by trigger events. T is a set of trigger events based on the human motion; they are the state transition conditions. T is denoted by

$$T = \{T_1, T_2, T_3\}. \tag{4}$$

When in state Q_{i-1} and the human motion triggered the trigger event T_i, the SRLs will execute the corresponding SRLs action a_i to coordinate with the human operator. The set of SRLs actions is defined as

$$a = \{a_1, a_2, a_3\}. \tag{5}$$

When SRLs action a_i is completed, the task state will transfer to the next state Q_i. The state transition function δ is defined by

$$\delta(Q_i, T_{i+1}) = (a_{i+1}, Q_{i+1}), i \in 0, 1, 2. \tag{6}$$

The overall FSM task model and the definition of the elements in the model are shown in Fig. 3. (i) Starting from the initial PS, when the human puts his hands up to place the ceiling, the trigger event T_1 is triggered to drive the SRLs to move upward just below the supporting points to be ready to support (SRLs action a_1). (ii) After action a_1, the task state changes to SS. When the ceiling position is aligned with the mounting holes (human hands stay still), the trigger event T_2 is triggered, which is the time SRLs need to reach the supporting

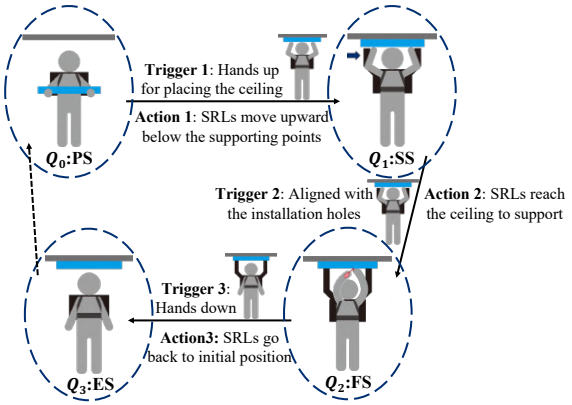

Fig. 3. State transition diagram in FSM model of the overhead task. The task model has four task states, three trigger events, and three SRLs actions. The task states are connected by black arrows, where the direction of the arrow represents the state transition direction. The trigger events of the human motion and SRLs actions are defined along the transition arrow.

points to hold the ceiling for the human (SRLs action a_2). (iii) Then FS is transitioned for the human to fix the ceiling. (iv) Finally, the human puts his hands down at the sides of the body (T_3) and the SRLs move from the ceiling (SRLs action a_3) to reach the resting positions and transition to ES. When the human is ready to begin another installation, the task state can be transitioned from ES to PS to initiate a new cycle.

FSM task model can identify the human intention to trigger the state transition and decide when to switch the SRLs control strategy. In addition, since the FSM model is a general description of the overhead tasks, the proposed model is suitable for overhead tasks with different parameters, which greatly enhances the task adaptability of human-SRLs system.

2) Trigger Event Detection and Task Parameter Estimation: According to the FSM task model, in human-SRLs collaboration, human motion can determine the task state transitions and guide the SRLs to take action. Therefore, trigger event detection is needed to identify the human intention from the human motion data. Human motion data can also provide information about the installation height and the supporting points of the SRLs, which is significant for SRLs control.

We propose a trigger event detection method based on real-time human motion data from the human motion capture system. The position of the human hands relative to the body segments and the velocity of the human hands are the two features used to detect trigger events. As shown in Fig. 3, in different states of the task, the position of the hands relative to the body is different. Taking the height of the waist and head of the human as the reference, the position of the hands relative to the body can be expressed with three integers as

$$R = \begin{cases} 1, & z_{hands,t} \geq z_{head,t} \\ 2, & z_{waist,t} \leq z_{hands,t} < z_{head,t} \\ 3, & z_{hands,t} < z_{waist,t} \\ 0, & \text{otherwise} \end{cases} \tag{7}$$

where $z_{hands,t}$, $z_{head,t}$, and $z_{waist,t}$ are the z coordinate of $\hat{P}^w_{hands,t}$, $\hat{P}^w_{head,t}$, and $\hat{P}^w_{waist,t}$, respectively; the subscript "hands" indicates that the condition is for both hands; the integers 1, 2, 3 indicate that the hands is working beyond the head, preparing in front of the chest and lowered down, respectively. For the state transition from FS to ES, in order to prevent accidental triggering during the FS, further judgment of the y position of the hands relative to the body is required, and the specific judgment condition is shown in Algorithm 1.

To accurately identify human intention, we detect the trigger event at the end of human action, at which point the human hands should be still. The generalized velocity of the hands can be determined by the range of positions of the hands within the nearest n time step. The threshold condition used to detect the stationarity of the hands is

$$\begin{aligned} \triangle(\hat{P}_{hands,t}) = \| &\max\{\hat{P}_{hands,t-n+1}, \hat{P}_{hands,t-n+2}, .., \hat{P}_{hands,t}\} \\ &- \min\{\hat{P}_{hands,t-n+1}, \hat{P}_{hands,t-n+2}, .., \hat{P}_{hands,t}\}\| \leq \epsilon \end{aligned} \tag{8}$$

where $\triangle$ is the generalized velocity calculator, $\hat{P}_{hands,t}$ can be the position vector or scalar component of the hands at time step t, and ϵ is a heuristically manually tuned threshold close to 0. The values n and ϵ are the trade-off between the detection robustness and the decision time delay. Increasing the values of n and ϵ result in a more robust but delayed detection. ϵ can also take the same form as $\hat{P}_{hands,t}$, either as a vector or a scalar. With the combination of the human hands' position and the stationary condition of hands, trigger events in the current task state can be detected accurately and timely.

When human limbs are in contact with the environment, the human motion data at a specific time allows to extract the task parameters. The installation height h of the ceiling can be estimated through trigger event T_1, when the human pre-place the ceiling to the expected height. Assuming that the height difference between the fingers and wrist is relatively constant when supporting the different heights of ceiling, the estimated ceiling height can be estimated by

$$h = \bar{z}^w_{hand,t} + h_f, \quad t = t_{T_1} \tag{9}$$

where $\bar{z}^w_{hand,t}$ is the average height of human hands in world frame; h_f is the assumed fixed height between wrist and ceiling, which can be determined by the experiment; and t_{T_i} is the time of trigger event T_i. At the same time, the target supporting point for the SRLs can be determined by setting an offset from the position of the human hands,

$$P^w_{support} = \hat{P}^w_{hand,t} + \eta, \quad t = t_{T_1} \tag{10}$$

where $P^w_{support}$ is the target supporting point in world frame, and $\eta \in \mathbb{R}^3$ is the offset between the supporting point and the human hand, which allows the SRLs to provide support on both sides of the hands.

Algorithm 1 shows the pseudo-code for the FSM task model. The trigger event detection condition in each task state and the estimated task parameters are shown. The position of the human hands during overhead tasks and the trigger event detection result are shown in Fig. 4.

C. SRLs Control Strategy

1) Motion Trajectory Generator: In human-SRLs overhead tasks, safety is the main issue for SRLs motion planning. In the

IEEE Robotics and Automation Letters (RA-L) paper, presented at ICRA 2024, Yokohama, Japan. Cite as RA-L paper.

Algorithm 1 FSM task model of overhead tasks.

INITIALIZE $Q \leftarrow PS, T \leftarrow \text{Nan}, a \leftarrow \text{Nan}$
while True **do**
  Get position of human segment $P_i[t]$
  if $Q = PS$ **and** $T = \text{Nan}$ **and** $R = 1$ **and** $\triangle(z_{hands}[t]) \leq \epsilon_z$ **then**
    $T \leftarrow T_1$
    Get installation height $h \leftarrow \bar{z}_{hand}[t] + h_f$
    Get supporting points $P_{support} \leftarrow P_{hands}[t] + \eta$
    Drive SRLs action $a \leftarrow a_1$
    $Q \leftarrow SS$
  if $Q = SS$ **and** $T = T_1$ **and** $R = 1$ **and** $\triangle(P_{hands}[t]) \leq \epsilon$ **then**
    $T \leftarrow T_2$
    Drive SRLs action $a \leftarrow a_2$
    $Q \leftarrow FS$
  if $Q = FS$ **and** $T = T_2$ **and** $R = 3$ **and** $\triangle(P_{hands}[t]) \leq \epsilon$ **and** $y_{Lhand} > y_{Lthigh}$ **and** $y_{Rhand} < y_{Rthigh}$ **then**
    $T \leftarrow T_3$
    Drive SRLs action $a \leftarrow a_3$
    $Q \leftarrow ES$
    Break

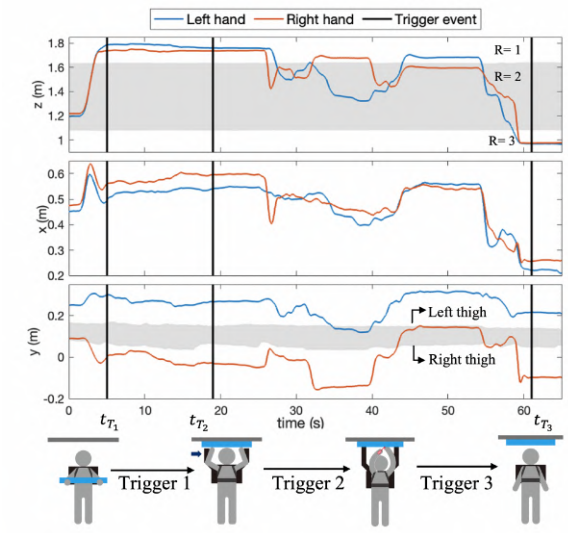

Fig. 4. Position of hands during human-SRLs collaboration with highlighted detected trigger events for one trial. In the first image, the position of the hands relative to the body segment is divided by gray shadows according to the position of the head and waist. From top to bottom, R is 1, 2, and 3, respectively. In the third image, the upper and lower edges of the gray shade represent the left and right thigh positions, respectively.

process of cooperating with the human, the motion trajectory of the end-effectors and links of SRLs cannot interfere with the human. Fig. 5(a) shows the block diagram of the trajectory generator of SRLs with RRT* algorithm [19] to plan the collision-free motion path of SRLs in high dimensional space.

The human limbs are approximated by cylinders with a radius of 5 cm, and the endpoints of these cylinders are determined by the real-time position of human limb segments. The initial position and the target position of SRLs in task space, represented in homogeneous form as T_{init} and T_{target}, are transformed into joint space coordinates $\theta_i, \theta_t \in \mathbb{R}^n$ (n is the number of DoFs of SRLs) by numerical inverse kinematics solver TRAC_IK [20]. In RRT*, the parent vertex θ_{parent} of a new sampling vertex θ_s is selected by FCL collision detection [21] with the approximated cylinders and minimizing path length. Once the predetermined planning time has been exceeded or the termination condition has been met, the motion path of the SRLs in the joint space is determined. The trajectory is sent to the controller after smoothing the segmented path using the multi-segment fifth-order Bezier curve.

2) Motion Controller: The collaboration control of the SRLs consists of different control strategies corresponding to the task state and state transition. In the human-SRLs collaboration, both human movement and sensor measurement errors can disturb the position control of SRLs in world frame, and the SRLs should show flexibility when interacting with the human and the ceiling to ensure safety. Especially in FS, when the SRLs support the ceiling, the up and down movement of the human hands during fixing will cause the shoulder to move up and down, which can interfere with the base position and makes it unable to keep supporting the ceiling. Therefore, we propose an admittance control with adjustable parameters to control the SRLs to behave like a spring-damping system,

$$B\dot{X}_e + KX_e = F_e, \tag{11}$$

where K, B are the stiffness and damping of the spring-damping system, respectively; $X_e = X - X_d$ is the displacement from the equilibrium position, $X \in \mathbb{R}^6$ is the Cartesian coordinate of the SRLs end-effector in its base frame, and X_d is the equilibrium position of the system; $F_e = F - F_d$ is the equivalent external force applied on the system, $F \in \mathbb{R}^6$ is the force at the end-effector, and F_d is the virtual force at the end-effector when the system is at the equilibrium position.

The use of different equilibrium forces F_d, stiffness K, and damping values B can allow to change the control characteristic of the SRLs for different task states and state transitions. Fig. 5(b) shows the block diagram of the proposed admittance control with end-effector force and position feedback loop. In this work, the ceiling is assumed to be fixed horizontally, and only the admittance control of SRLs in the z direction is considered.

For SRLs actions a_1 and a_3, the SRLs need to behave in pure damping mode ($K = 0$, $F_d = 0$) to ensure safety in the case of an accidental collision with the human. This means that the motion velocity of the SRLs is proportional to the external force, so that the SRLs will correct the current expected trajectory and move in the direction of the external force. For the SRLs action a_2, after the human confirms the ceiling position, the SRLs need to move up to contact with the ceiling with flexibility ($F_d = 0$). The calculated end-effector force of the SRLs can be used to detect the contact and to correct the estimated error of the installation height.

When the SRLs come into contact with the ceiling, x_d is set to the current position and F_d will increase linearly towards the maximum contact force F_{max}. When F_d increases, the equivalent force F_e on the spring-damping system decreases,

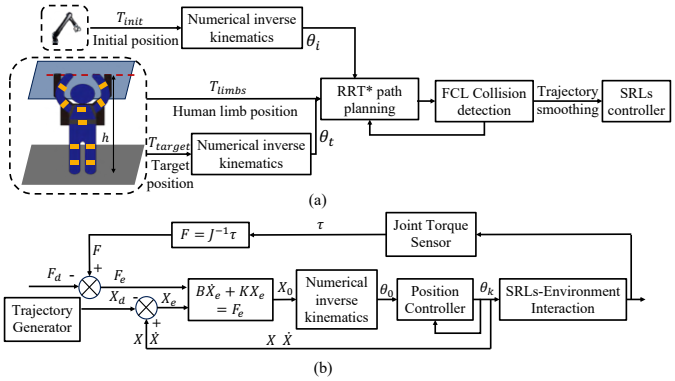

Fig. 5. Block diagram of SRLs control strategy. (a) Block diagram of trajectory generator of SRLs in joint space. (b) Block diagram of SRLs admittance control. The force F at the end-effector is calculated by the joint torque through the inverse force jacobian. X_d in the SRLs base frame can be obtained from the trajectory generator by forward kinematics and F_d is meant to be the expected force at X_d.

TABLE I
COMBINATIONS OF PARAMETERS IN EXPERIMENT

Experiment	Subject	Height (m)	h (m)	h_n
I	1	1.81	1.93	0.79
II	1	1.81	1.98	0.89
III	1	1.81	2.03	0.99
IV	2	1.74	1.88	0.94
V	2	1.74	1.93	1.05
VI	2	1.74	1.98	1.15

causing the SRLs to move upwards, resulting in an increase of the contact force to F_d. When the contact force F exceeds a certain threshold F_{thr}, the task state switches to FS. In FS, when the human limbs are lowered causing the SRLs to release from supporting the ceiling, the force F decreases and the equivalent force F_e decreases as well. As the force F on the SRLs decreases, the SRLs will also move upwards to increase the contact force. By adjusting appropriate stiffness, the proposed admittance control enables the SRLs to have corresponding stable contact force F at each position X,

$$F = F_{max} - K(X - X_d). \tag{12}$$

In order to keep supporting when the human is fixing the ceiling, the expected minimum contact force F_{min} for each robotic arm is set to be half the weight of the ceiling plus a safety margin force F_{margin}, denoted by

$$F_{min} = \frac{mg}{2} + F_{margin}. \tag{13}$$

Then the feasible region of the contact force during FS is that the contact force in the z direction of SRLs end-effector is not less than the expected minimum contact force.

III. EXPERIMENT AND RESULTS

In this section, the experiment designed to verify the effectiveness of the proposed task-based human-SRLs collaboration control in overhead tasks with different task parameters is presented. The experimental protocol was approved by the Institutional Review Board at Southern University of Science and Technology (approval number: 20220031, date: 2022/2/25).

TABLE II
PARAMETERS OF THE PROPOSED METHOD IN THE EXPERIMENT

Eqs. (8) and (9)	$n = 10$, $\epsilon = [0.005, 0.005, 0.01]$ m, $h_f = 0.2$ m		
Eqs. (10)	$\eta_{left} = [-0.15, 0.1, 0.2]$ m, $\eta_{right} = [0.1, -0.15, 0.2]$ m		
Eqs. (11)	Task stage	K (N/m)	B (Ns/m)
	a_1 & a_3	0	30
	a_2 & FS	500	50
Eqs. (12) and (13)	$F_{max} = 30$ N, $F_{min} = 8$ N, $F_{margin} = 6$ N		
Others	$F_{thr} = 20$ N		

A. Experimental Protocol

The prototype hardware configuration and the sensing system of the human-SRLs system are depicted in Fig. 1. The SRLs consist of two 6-DoF robotic arms (Kinova Gen2, Kinova, CA) with a maximum reach of 985 mm, suitable for overhead tasks performed by adults. The SRLs are attached to the mounting base by inserting two sleeves, which allows for secure and stable attachment. The base of the SRLs is then mounted on the back of the human operator via a backpack belt. The total weight of the prototype composed by the SRLs and the mounting base is 14 Kg, including the 4.4 Kg for each robotic arm. A 3D-printed spherical end-effector is gripped by the fingers of the robotic arm to ensure effective and stable support in different tool poses. A mini PC (NUC, Intel, USA) based on Linux OS is fixed on the mounting base of SRLs and runs the controller codes. Robot Operating System (ROS) is adopted to connect the SRLs and the sensing system.

Two male subjects of different heights (subject 1: age 21 years; height 181 cm; weight 75 Kg; subject 2: age 27 years; height 174 cm; weight 72 Kg) were invited as the human operator to participate in the experiment. Prior to conducting the experiment, the participants were given a thorough explanation of the task process and the collaboration allocation between the human and the SRLs. In order to ensure the participants were adequately prepared for the experiment, a pre-experiment was conducted, involving wearing the prototype to acclimate them to the weight and having two subjects collaborate with each other ten times to familiarize themselves with the collaboration process of the task. In the experiment, subjects were required to collaborate with the SRLs to fix the ceiling at three different installation heights, three trials for each condition. The same ceiling height may present different challenges for humans of different heights. To standardize this measurement, we determine the normalized installation height h_n by calculating the ratio of the distance between the human shoulders and the ceiling h_s to the average length of the human arms l_{arm}, denote by

$$h_n = \frac{h_s}{l_{arm}}. \tag{14}$$

This normalized installation height is independent of the human height, providing a consistent and accurate measure of task parameters of different installation heights. Six different normalized installation heights can allow to fully demonstrate the effectiveness of the proposed method in different task parameters, as shown in Table. I. For safety reasons, we used a foam board (400 g) with four mounting holes to represent the

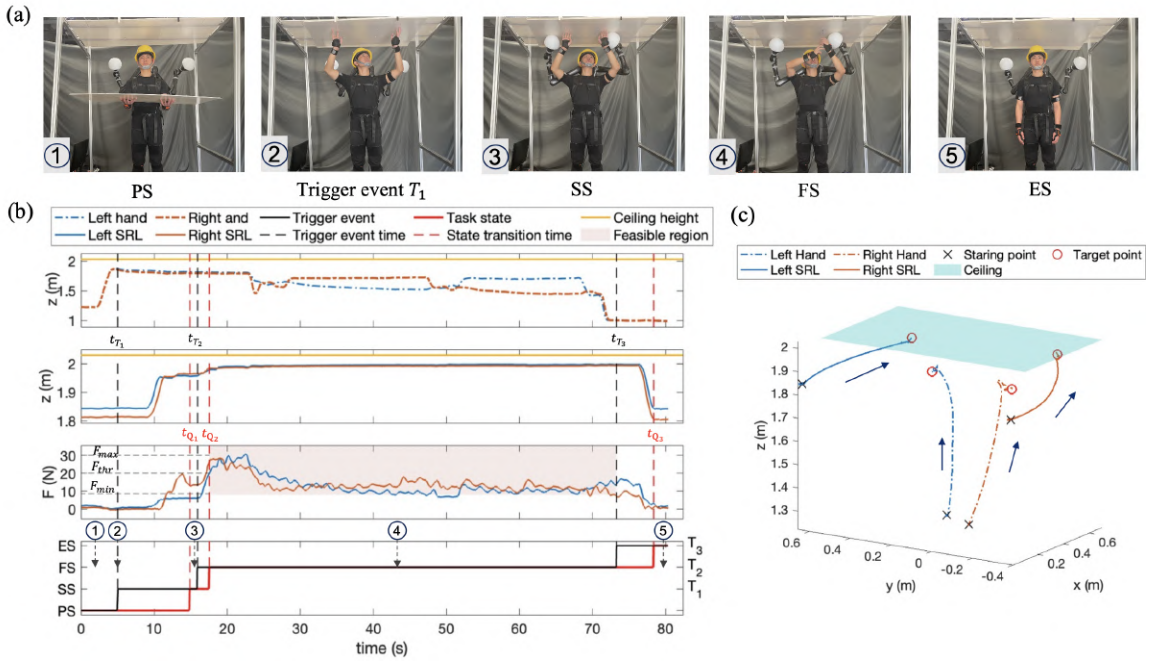

Fig. 6. Results of human-SRLs collaboration in overhead tasks for subject 1 in Experiment III. (a) Snapshots of human-SRLs collaboration process. (b) The position of the human hands and the SRLs end-effectors (z direction in world frame), the end-effector force of SRLs (z direction in world frame), and the trigger events and task states in collaboration process, respectively. The black and red solid lines represent the trigger events and task states, and the corresponding red and black dotted lines represent the moment of trigger event detection t_{T_i} and task state transition t_{Q_i}, respectively. (c) The 3D trajectories of the human hands and the end-effectors of SRLs from PS to SS. The starting points, target points, and directions of the trajectory are marked out.

real ceiling. During the installation process, both subjects can choose the appropriate supporting posture according to their habits. When at least two holes on the diagonal are fixed, the ceiling could be considered to be installed successfully. Table. II displays some parameters mentioned in the proposed methods for the experiment.

B. Experiment Results

Considering the six experimental conditions, the ceiling was successfully fixed in all the 18 attempts. During the experiment process, the proposed method can accurately and timely identify the human intention to detect trigger events and estimate the current task parameter to successfully generate the SRLs motion trajectories and switch the corresponding control parameters. The average time for the two subjects with the SRLs to complete the overhead tasks was very similar, with times of 80.8 $\pm$ 12.1 s and 85.3 $\pm$ 11.1 s, respectively. In comparison, the average completion time for human-human collaboration was 46.2 $\pm$ 6.2 s, while a single person was unable to complete the task. These comparisons indicate that although SRLs may not be as efficient as human-human collaboration, they can help save labor costs and enhance human operating capabilities in confined spaces where large commercial devices and multiple humans cannot access. To illustrate the results, the result of one trial in Experiment III will be presented in detail, as the results from the other 5 experiments, which varied in human height and installation height, were found to be similar.

Fig. 6 shows the human-SRLs collaboration process for subject 1 in Experiment III, in which the subject fixed the ceiling at 2.03 m. It can be observed in Fig. 6(a) that the SRLs can coordinate with human autonomously within the framework of the task model. The five images from left to right are PS state, trigger event T_1, SS state, FS state, and ES state of the task.

Fig. 6(b) presents a comprehensive examination of the human-SRLs collaboration process by displaying the data in a detailed and informative manner. Fig. 6(b) shows the plot of position, force, trigger events, and task states during the whole process of the collaboration. The task state and the trigger events marked by the numbers on the fourth subplot correspond to the snapshot numbers. It is possible to gain insights into the task process by observing the curve of the position of the human hands and the motion and force of the SRLs over time during the entire task process. To begin with, when trigger event T_1 is detected, the estimated installation height obtained from the average human hands' positions is 2.022 m, which is very close to the actual height. It can be seen that in SRLs action a_1, the SRLs follow the planned trajectories to the supporting points below but not to contact with or beyond the ceiling. Subsequently, in SRLs action a_2, the SRLs move upward to support the ceiling after t_{T_2}. As parameter F_d increasing linearly to the maximum contact force, the supporting force increases linearly around $30N$, during the time when the force of both the left SRL and right SRL exceed the F_{thr}, state transfer to FS, as shown in the third subplot of Fig. 6(b). In FS, the SRLs behave like a spring-damping system. When human operator supports the ceiling with the SRLs, the SRLs are in its equilibrium position with maximum force to the ceiling. When the human hands are

lowered, the SRLs stretch to still maintain contact with the ceiling, where the contact force is reduced accordingly but still in the feasible region ($F \geq 8$ N). Additionally, the fact that the height of SRLs in world frame remains constant in FS can also verify the conclusion that the SRLs are continuously supporting the ceiling.

Fig. 6(c) demonstrates the 3D trajectories of the human hands and the SRLs from PS to the time when task state transition to FS. The motion trajectories of SRLs are determined by the human limbs and task model to ensure the safety of the collaboration. It can be observed that the trajectories of SRLs will not interfere with the human limbs and the ceiling during the collaboration process.

IV. Discussion and Conclusion

In this study, an effective and autonomous human-SRLs collaboration control method was proposed for complex tasks with different task parameters. This paper demonstrates the proposed method for overhead tasks, which encompass a range of complex and demanding operations in industrial settings such as aircraft compartments.

The proposed method offers several key advantages. Firstly, it establishes a clear communication channel for task knowledge and intention between the human and SRLs. In the existing literature, the control of SRLs relies on the active commands [9]–[11] and teaching data [12]–[14], which can be challenging to apply in complex collaboration processes and varying task parameters. In contrast, by utilizing real-time human motion data and a task model, SRLs are able to respond to the human's actions in a collaboration manner. This autonomous coordination can effectively reduce the cognitive load, as they are not required to control both their own limbs and SRLs simultaneously. The second advantage is its ability to adapt to different task parameters and ensure the safety of human-SRLs collaboration. Through experiments with six different installation heights, it was determined that the human motion data at the certain moment (trigger event T_1) can be used to estimate the installation height with an absolute error of less than 2 cm. This eliminates the need for measuring the height and position of the ceiling prior to installation, increasing the method's adaptability. Additionally, the planned motion trajectories based on the ceiling height and human support position, and the admittance control with adjustable parameters ensure the safety of human-SRLs collaboration.

One of the limitations lies in the generalization of this method. For other applications, it is necessary to create corresponding task models and set appropriate state transition conditions specific to the task workflow. Although recent advances [22] in neuroscience have demonstrated the potential for controlling SRLs using brain-machine interfaces, which could eliminate the need for task models by directly controlling SRLs via neural DoFs, it is still in its infancy. The development of a unified control framework for SRLs across diverse and complex tasks is unlikely to be feasible in the short term. Thus, from a practical standpoint, combining task models and human intention for autonomous collaboration remains a valuable area of study. Future work includes expanding the method's application to other complex human-SRLs tasks.

References

[1] J. Eden, M. Bräcklein, J. Ibáñez, D. Y. Barsakcioglu, G. Di Pino, D. Farina, E. Burdet, and C. Mehring, "Principles of human movement augmentation and the challenges in making it a reality," *Nature Communications*, vol. 13, no. 1, p. 1345, 2022.

[2] D. Prattichizzo, M. Pozzi, T. Lisini Baldi, M. Malvezzi, I. Hussain, S. Rossi, and G. Salvietti, "Human augmentation by wearable supernumerary robotic limbs: Review and perspectives," *Progress in Biomedical Engineering*, vol. 3, no. 4, p. 042005, 2021.

[3] M. Hao, J. Zhang, K. Chen, H. Asada, and C. Fu, "Supernumerary robotic limbs to assist human walking with load carriage," *Journal of Mechanisms and Robotics*, vol. 12, no. 6, p. 061014, 2020.

[4] M. A. Gull, S. Bai, and T. Bak, "A review on design of upper limb exoskeletons," *Robotics*, vol. 9, no. 1, p. 16, 2020.

[5] C. Ahmadizadeh, M. Khoshnam, and C. Menon, "Human machine interfaces in upper-limb prosthesis control: A survey of techniques for preprocessing and processing of biosignals," *IEEE Signal Processing Magazine*, vol. 38, no. 4, pp. 12–22, 2021.

[6] Z. Bright and H. Harry Asada, "Supernumerary robotic limbs for human augmentation in overhead assembly tasks," in *Robotics: Science and Systems XIII*. Robotics: Science and Systems Foundation, 2017.

[7] F. Cini, T. Banfi, G. Ciuti, L. Craighero, and M. Controzzi, "The relevance of signal timing in human-robot collaborative manipulation," *Science Robotics*, vol. 6, no. 58, p. eabg1308, 2021.

[8] J. W. Guggenheim and H. H. Asada, "Inherent haptic feedback from supernumerary robotic limbs," *IEEE Transactions on Haptics*, vol. 14, no. 1, pp. 123–131, 2021.

[9] P. Kieliba, D. Clode, R. O. Maimon-Mor, and T. R. Makin, "Robotic hand augmentation drives changes in neural body representation," *Science robotics*, vol. 6, no. 54, p. eabd7935, 2021.

[10] J. Guggenheim, R. Hoffman, H. Song, and H. H. Asada, "Leveraging the human operator in the design and control of supernumerary robotic limbs," *IEEE Robotics and Automation Letters*, vol. 5, no. 2, pp. 2177–2184, 2020.

[11] F. Parietti and H. H. Asada, "Independent, voluntary control of extra robotic limbs," in *2017 IEEE International Conference on Robotics and Automation*. IEEE, 2017, pp. 5954–5961.

[12] B. L. Bonilla and H. H. Asada, "A robot on the shoulder: Coordinated human-wearable robot control using coloured petri nets and partial least squares predictions," in *2014 IEEE International Conference on Robotics and Automation*. IEEE, 2014, pp. 119–125.

[13] B. Llorens- Bonilla, F. Parietti, and H. H. Asada, "Demonstration-based control of supernumerary robotic limbs," in *2012 IEEE/RSJ International Conference on Intelligent Robots and Systems*. IEEE, 2012, pp. 3936–3942.

[14] F. Y. Wu and H. H. Asada, "Implicit and intuitive grasp posture control for wearable robotic fingers: A data-driven method using partial least squares," *IEEE Transactions on Robotics*, vol. 32, no. 1, pp. 176–186, 2016.

[15] Y. Wu, P. Balatti, M. Lorenzini, F. Zhao, W. Kim, and A. Ajoudani, "A teleoperation interface for loco-manipulation control of mobile collaborative robotic assistant," *IEEE Robotics and Automation Letters*, vol. 4, no. 4, pp. 3593–3600, 2019.

[16] W. Kim, L. Peternel, M. Lorenzini, J. Babič, and A. Ajoudani, "A human-robot collaboration framework for improving ergonomics during dexterous operation of power tools," *Robotics and Computer-Integrated Manufacturing*, vol. 68, p. 102084, 2021.

[17] J. Luo, Z. Gong, Y. Su, L. Ruan, Y. Zhao, H. H. Asada, and C. Fu, "Modeling and balance control of supernumerary robotic limb for overhead tasks," *IEEE Robotics and Automation Letters*, vol. 6, no. 2, pp. 4125–4132, 2021.

[18] M. Schepers, M. Giuberti, and G. Bellusci, "Xsens mvn: Consistent tracking of human motion using inertial sensing," *Xsens Technol*, vol. 1, no. 8, 2018.

[19] S. Karaman and E. Frazzoli, "Sampling-based algorithms for optimal motion planning," *The International Journal of Robotics Research*, vol. 30, no. 7, pp. 846–894, 2011.

[20] P. Beeson and B. Ames, "TRAC-IK: An open-source library for improved solving of generic inverse kinematics," in *2015 IEEE-RAS 15th International Conference on Humanoid Robots (Humanoids)*. IEEE, 2015, pp. 928–935.

[21] J. Pan, S. Chitta, and D. Manocha, "FCL: A general purpose library for collision and proximity queries," in *2012 IEEE International Conference on Robotics and Automation*. IEEE, 2012, pp. 3859–3866.

[22] C. I. Penaloza and S. Nishio, "Bmi control of a third arm for multitasking," *Science Robotics*, vol. 3, no. 20, p. eaat1228, 2018.